IEEE Access
Multidisciplinary | Rapid Review | Open Access Journal

Received April 1, 2022, accepted April 27, 2022, date of publication May 3, 2022, date of current version May 11, 2022.

Digital Object Identifier 10.1109/ACCESS.2022.3172353

Research on Purging and Ventilation Progress of Positive-Pressure Explosion-Proof Motor

WENHUI LIU, MENGMENG AI, LISHEN XU, AND HAN GOU
College of Electrical and Electronic Engineering, Harbin University of Science and Technology, Harbin 150080, China
Corresponding author: Mengmeng Ai (aimengmeng@hrbust.edu.cn)

This work was supported by the National Natural Science Foundation of China under Grant 52077047.

ABSTRACT In order to solve the problems of time-consuming, high-cost and poor safety in the purging and ventilation progress test of positive pressure explosion-proof motor, the multi-component fluid theory is introduced to analyze the positive-pressure explosion-proof motor. According to the basic explosion-proof principle and key problems of purging and ventilation progress simulation of positive-pressure explosion-proof motor, the explosion-proof finite element model of the motor is established, and the purging and ventilation progress of the motor is simulated and analyzed by multi-component fluid theory. By controlling the concentration of He (helium), the explosive environment and the purging process of the motor can be achieved, and it can be known whether there is a purging dead angle in the motor by observing the transient concentration of each component, which enhances the safety performance of the motor. Then the accuracy of the simulation is verified by experiments. Finally, based on the observation of the fluid components in the original motor, an optimization scheme of changing the intake pipe is proposed, which can improve the efficiency of purging and enhance the reliability of the motor.

INDEX TERMS Positive-pressure motor, purging and ventilation progress, multi-component transient concentration field.

I. INTRODUCTION

In recent years, due to the rapid development of natural gas, petroleum, coal, and other industries, the demand for explosion-proof motors is increasing day by day. The positive pressure explosion-proof motor with the high power, high safety, and other remarkable characteristics is the main power component of the driving fan, water pump, compressor, and other equipment, and its market share is also significantly increased [1]. There are two key technologies of positive pressure explosion-proof motor. One is to maintain the positive pressure value, which is generally 1.5 times the maximum pressure generated on the equipment shell and pipeline; The second is the ventilation and purging process, which is directly related to the purging time and amount, and also affects whether there is a purging dead angle after the motor is purged, resulting in potential safety hazards.

At present, the purging and Ventilation Progress of explosion-proof motor is mainly verified by a large number of reliability tests, which will consume a lot of time and cost. Considering the sake of economy and time, it is often not to carry out reliability tests on all motors but to take appropriate samples from them according to certain principles or examples for tests, and the test results of these samples are used to judge whether the explosion-proof level of this batch of motors meets the explosion-proof requirements. In this way, the motor will have a certain probability of disqualification [2]. Because the application history of positive-pressure explosion-proof motor is short, and the area to be analyzed for purging and Ventilation Progress is a multi-component concentration field composed of air and explosive gas, not only the density and viscosity of multi-component should be considered, but also the whole analysis process is a transient process with the time change. Because the simulation analysis of purging and ventilation process of positive pressure explosion-proof motor is a complex and difficult subject. At present, there is little research on its safety performance simulation in the field of motor. However, the research of multi-component concentration field in the field of air pollution diffusion is quite common, which has certain reference significance. The main method of analysis is to establish a diffusion model of pollutants in the air and

The associate editor coordinating the review of this manuscript and approving it for publication was Padmanabh Thakur.

simulate the distribution of pollutants over time. R. Pokhrel and other scholars have studied the air quality in Incheon area of South Korea, where the pollution is increasing day by day. They have analyzed the diffusion of pollution gas emitted by ocean-going ships under the action of ocean airflow, which plays a promoting role in improving the air pollution level in the area [3]. A. Monteiro has studied the Inland diffusion of high concentration ozone in the central region of Portugal under the action of the sea breeze. The results show that the pollution source can diffuse inland up to 30 km [4]. Zhang Jingui has studied the pollution diffusion of automobile exhaust in the tunnel, and the analysis shows that the exhaust will form a large number of piles near the ground without ventilation, and a high-speed wind belt will be formed when the automobile moves, which plays a key role in the diffusion of exhaust [5]. Huang Yuandong has studied the influence of buildings around the street intersection on the airflow and pollution diffusion, and the research shows that a reasonable building layout is conducive to the rapid diffusion of pollution gas [6]. Li Ting studied the diffusion of formaldehyde in the room, and comprehensively considered the influence of existing indoor formaldehyde concentration, formaldehyde release speed, indoor wind speed change, and other factors. The conclusions are of guiding significance for eliminating and controlling formaldehyde pollution [7]. Xiao Mingming has studied the diffusion of radioactive pollutants in the event of an accident at a nuclear power plant. Considering the influence of the decay rate of radioactive pollutants, airflow change, air humidity and other factors on the diffusion rate, a diffusion model for radioactive pollutants has been established based on the Gaussian model, the research results can provide guidance for the emergency response plan of a nuclear power plant [8].

In conclusion, at present, scholars have made a more in-depth study on the multi-component concentration field in the aspects of air pollution diffusion, meteorology, chemical industry, medicine, and so on, while no relevant reference has been found in the aspect of the electrical machine. The explosion-proof area of the motor is a single-phase gas composed of oxygen, nitrogen, hydrogen, or methane. There are no solid and liquid components, which belong to the category of multi-component concentration field. Therefore, the simulation analysis of the purging and Ventilation Progress of the motor can reference from the research results of air pollution diffusion, and apply the theory, model, and method to the field of explosion-proof motor, which should be able to achieve the simulation analysis of purging and Ventilation Progress of explosion-proof motor.

This paper takes a 6.5 MW positive pressure explosion-proof motor as an example, according to the basic explosion-proof principle of positive-pressure explosion-proof motor and the key problems of purging and Ventilation Progress simulation of positive-pressure explosion-proof motor. The multi-component fluid theory is applied to the positive-pressure explosion-proof motor. He is used as the simulated explosive gas, and the finite element method is used to simulate the purging and Ventilation Progress of the motor. The time and volume of purging of the motor are obtained. Through the concentration nephogram of each part, we can know whether there is a purging dead angle in the motor. After the simulation analysis, the results are compared with the explosion-proof tests to verify the simulation accuracy. Finally, the layout of the intake pipe is improved to increase the purging efficiency.

II. METHODOLOGY

There are combustibles such as hydrogen and acetylene in the environment of positive-pressure explosion-proof motor, and there may be spark, corona, high temperature and other ignition sources in the motor, which has already met the necessary conditions for explosion, if no additional measures are taken, it is easy to explode. The positive-pressure explosion-proof motor is filled with a certain amount of protective gas in the motor, so that the ignition source inside the motor is in the protective gas, and the pressure of the protective gas inside the motor is always higher than the pressure of the combustible gas in the surrounding environment, so as to prevent the combustible gas from entering the motor, effectively isolate the ignition source from the combustible, so as to avoid explosion.

A. THE KEY TECHNOLOGY OF POSITIVE PRESSURE EXPLOSION-PROOF MOTOR

(1) Maintain positive-pressure. When the positive-pressure explosion-proof motor is in normal operation, it is necessary to keep a certain positive pressure value inside the equipment, which requires the equipment to have sufficient mechanical strength and sealing, so as to avoid damaging deformation and pressure leakage. This link is to monitor the internal pressure of the motor in real-time through the positive-pressure system device. When the pressure is insufficient, the leakage compensation will be carried out, and there will be alarm promptly when there is a fault. At present, this technology has been very mature [9].

(2) Purging and ventilation. When the positive-pressure explosion-proof motor starts normally, there may be combustible gas inside the motor. Therefore, before the motor starts, the inert gas or clean air shall be purged into the motor to discharge the combustible gas inside the motor, and this process is called the purging and ventilation process. The purging and ventilation process of a positive-pressure explosion-proof motor is a very important link. It is necessary to ensure that the explosive gas concentration in all positions of the motor is lower than the explosion limit concentration, and there is no dead angle. At present, it is ensured by tests that many monitoring points are set in the motor casing, and multi-point measurement is carried out after the purging and ventilation. However, this method can only monitor the explosive gas concentration near the motor casing, and the explosive gas concentration inside the motor can not be guaranteed, which has certain limitations. In addition, it often appears that the concentration value of most monitoring points has

reached the standard in the test, but only one monitoring point has not reached the standard. To reach the standard, a lot of purging and ventilation time needs to be increased, and a lot of purging and ventilation resources and time are wasted. The main reason for this is that the layout of the purging pipeline is unreasonable. Therefore, the simulation research on the purging and Ventilation Progress of positive-pressure explosion-proof motor should mainly focus on the simulation analysis of the purging and ventilation process, which can obtain the explosive gas concentration value in all positions of the motor, so that there is no dead angle of purging in the motor, making up for the lack of explosion-proof test. In addition, the reasonable arrangement of purging pipelines can save a lot of purging resources and time [10].

B. MATHERMATICAL MODEL

All matter flows must satisfy the conservation laws, including the conservation laws of mass and momentum. If there are different components in the matter, the system should also meet the conservation law of components. If the Reynolds number of the calculated region is too large, the flow state of matter will belong to turbulence, that is to say, the transport equation of turbulence should be satisfied [11]–[13].

C. LAW OF CONSERVATION OF MASS

Whether the fluid in the motor is stable or unstable, it meets the mass conservation equation:

$$\frac{\partial \rho}{\partial t} + u\frac{\partial(\rho u)}{\partial x} + v\frac{\partial(\rho v)}{\partial x} + w\frac{\partial(\rho w)}{\partial x} = 0 \tag{1}$$

where ρ is the density; u, v, w is the velocity component in the x, y, z direction.

D. LAW OF CONSERVATION OF MOMENTUM

Any form of fluid flow must satisfy the law of conservation of momentum. That is to say, the rate of change of fluid momentum of any micro element to time is always equal to the sum of various forces such as pressure, viscous stress, and volume force exerted on the micro element. According to Newton's second law, the conservation equation of momentum in \ emph {x, y, z} direction can be derived as shown in Eq. (2).

$$\left.\begin{aligned}
&\frac{\partial(\rho u)}{\partial t} + \frac{\partial(\rho uu)}{\partial x} + \frac{\partial(\rho uv)}{\partial y} + \frac{\partial(\rho uw)}{\partial z} \\
&= -\frac{\partial p}{\partial x} + \frac{\partial \tau_{xx}}{\partial x} + \frac{\partial \tau_{yx}}{\partial y} + \frac{\partial \tau_{zx}}{\partial z} + F_x \\
&\frac{\partial(\rho v)}{\partial t} + \frac{\partial(\rho vu)}{\partial x} + \frac{\partial(\rho vv)}{\partial y} + \frac{\partial(\rho vw)}{\partial z} \\
&= -\frac{\partial p}{\partial y} + \frac{\partial \tau_{xy}}{\partial x} + \frac{\partial \tau_{yy}}{\partial y} + \frac{\partial \tau_{zy}}{\partial z} + F_y \\
&\frac{\partial(\rho w)}{\partial t} + \frac{\partial(\rho wu)}{\partial x} + \frac{\partial(\rho wv)}{\partial y} + \frac{\partial(\rho ww)}{\partial z} \\
&= -\frac{\partial p}{\partial z} + \frac{\partial \tau_{xz}}{\partial x} + \frac{\partial \tau_{yz}}{\partial y} + \frac{\partial \tau_{zz}}{\partial z} + F_z
\end{aligned}\right\} \tag{2}$$

where ρ is the pressure on the fluid micro element; τ_{xx}, τ_{xy} and τ_{xz} are the components of the viscous stress, and along the x, y, z direction; F_x, F_y and F_z are the volume force on the micro element.

E. CONSERVATION LAW OF COMPONENTS

The concentration field of the positive-pressure explosion-proof motor studied in this paper is a multi-component fluid area composed of various gases, which need to meet the conservation law of components. That is, the physical parameters of the fluid in the calculation area are determined by the physical properties of each component fluid and its mass fraction, and the sum of the mass fraction of each component is equal to 1 [14].

$$\sum_{i=1}^{n} Y_i = 1 \tag{3}$$

where Y_i is the mass fraction of each component fluid; n is the component fraction, equal to 3(He, O2, N2);, the fluid density of each component is 0.1625 kg/m3, 1.2999 kg/m3 and 1.138 kg/m3; the hydrodynamic viscosity of each component is 1.99e^{-5} kg/m·s, 1.919 e^{-5} kg/m·s, 1.663e-5 kg/m·s.

F. BASIC TRANSPORT EQUATION OF TURBULENCE

The Reynolds equation is:

$$R_e = \rho \cdot \nu \cdot / \beta \tag{4}$$

where ρ is the density, equal to 1.29 kg/m^3, νvis the flow rate, equal to 30 m/s, d is the pipe diameter, equal to 0.042 m, β is the viscosity, equal to 1.789e^{-5} kg/m·s,;

Because of the complexity of the wind path and the changeability of the moving track, the flow of the fluid often exists in the form of turbulence. At present, the standard $k-\varepsilon$ model is often used to analyze the turbulent flow state, as shown in Eq. (5).

$$\frac{\partial(\rho\phi)}{\partial t} + div(\rho V\phi) = div(\Gamma grad\phi) + S \tag{5}$$

where V, ϕ is general variables, Γ is the diffusion coefficient, S is the source term, ρ is the fluid density.

G. SAMPLING PROTOTYPE

The prototype is shown in Fig. 1.

The basic parameters of the motor are shown in Tab. 1.

Because the purging and ventilation process is only related to the fluid flow in the motor, the forced fan, bearing, junction box, and other components are omitted in the modeling. The stator, rotor, and cooling pipe inside the motor are drawn in detail. According to the actual structure of the motor, the solution model established is shown in Fig. 2.

The transverse section and longitudinal section defined in Fig. 2 and points A, B, C, D, and E are used for simulation analysis and explanation. On the axial section, points F, G, H, I, and J correspond to points A B, C, D, and E.

H. BASIC ASSUMPTIONS

To establish the model of the motor, the following assumptions are made [15]–[17]:

(1) The chemical reactions among multi-components are not considered.

FIGURE 1. The actual prototype of positive-pressure explosion-proof motor.

TABLE 1. The basic parameters of the prototype.

Parameters	Rated value
Power (MW)	6.5
Pole number	20
Voltage (kV)	11
Frequency (Hz)	50
Stator Outer Diameter (mm)	2600
Stator Inner Diameter (mm)	2200
Rotor Outer Diameter (mm)	2192
Rotor Inner Diameter (mm)	1900
Number of stator slots	180
Number of rotor slots	220
Iron Core length (mm)	1100
Ventilation duct number	11
The Length * High of Iron Core (mm)	3000*1100
Specification of Cooling Pipe (mm)	φ23×1.5 c
Number of cooling pipes	202
Number of internal fans	2
Stator Slot Type 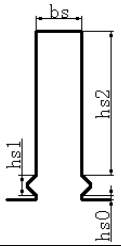	Rotor Slot Type 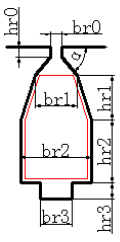
Protection level	IP55
Explosion proof grade	ExpxdeIIT3 Gb
Installation site	Zone 2 (IIC)、Outside

(2) The temperature of the gas does not change during the whole process.

(3) When the gas in the motor is under normal pressure, the influence of buoyancy and gravity in the fluid domain is ignored.

(4) The velocity of the fluid is far less than that of sound, which means that the fluid in the motor is treated as an incompressible fluid.

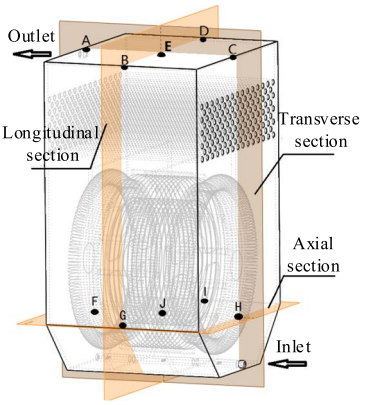

FIGURE 2. The physical model of positive-pressure explosion-proof motor.

I. BOUNDARY CONDITIONS

1. Transient simulation calculation of simulated explosive environment

(1) The installation site of the motor is zone 2 (IIC), the main explosive gas is H_2 and C_2H_2, and He is used as the simulated explosive gas (He is often used as the simulated explosive gas in the explosion-proof test, because the density of He is similar to that of H_2, and it is inert gas).

(2) At the beginning, the inside of the motor is air.

(3) The He with the concentration of 100% is blow into the motor inlet. The speed inlet is adopted and the speed value is 30 m/s. The pressure outlet is adopted.

(4) The end condition of calculation is that the concentration of He at each sampling point is not less than 70% (according to the requirements of explosion-proof standard).

2. Transient simulation calculation of purging and ventilation

(1) Combined with the real test process, the motor will be "purged" after "simulated explosive environment", so the end state of "simulated explosive environment" is taken as the initial state of the purging transient calculation.

(2) The air with the concentration of 21% O_2 and 79% N_2 (The air also contains rare gases, CO_2, water vapor and impurities, but their volume fractions add up to less than 1%. In order to simplify the calculation, they are ignored and their volume fractions are attributed to N_2.) is blown into the motor inlet. The speed inlet is adopted and the speed value is 30m /s. The pressure outlet is adopted.

(3) The end condition of calculation is: the concentration of He at each sampling point is not higher than 1% (according to the requirements of explosion-proof standard).

J. THE SIMULATION MODEL ESTABLISHMENT

According to the motor model, basic assumptions and boundary conditions, the simulation model is established by using the finite element analysis software ANSYS, and its gird mesh is shown in Fig.3

In Fig3, the octree method is also used for grid division. The mesh unit is 19.93 million and the number of nodes is 3.52 million

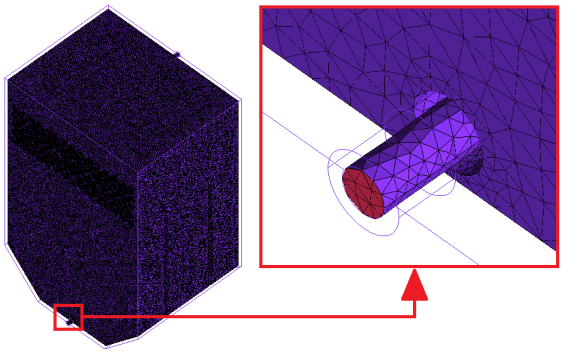

FIGURE 3. The gird mesh of model.

K. THE EXPERIMENTAL PLATFORM

Purging and ventilation test is the difficulty of the explosion-proof test, which not only needs a long test time and uses a large number of expensive He, but also often occurs that the He concentration at some test points does not meet the explosion-proof requirements. The test position set during the explosion-proof test of purging and ventilation of the prototype is shown in Fig. 4(a). There are 6 places on the frame and 4 places on the cooler. Fig. 4(b) is to measure the concentration of each point through the instrument. When the concentration of He in all test points reaches more than 70%, the fresh air is purged. When the concentration of He in all test points drops below 1%, the purge time and minimum purge volume are obtained.

III. SIMULATION ANALYSIS

It is necessary to maintain a certain positive-pressure value inside the positive-pressure explosion-proof motor in the operation, thus the process of purging and ventilation needs to be completed before starting the motor. The inert gas or clean air is blown into the motor, and flammable gases inside the motor are exhausted to the outside of the motor, which can reduce the hidden danger of motor safety [18]. Since the maximum velocity in the system in this paper will not exceed 30m / s, which belongs to the field of low speed, the separated solver in fluent is adopted. Time step size is 0.01s, and the max Iterations/time step is 20.

A. SIMULATED EXPLOSIVE ENVIRONMENT

According to Fig. 5, when t = 1680s, the He concentration of sampling points in the calculation model reaches more than 70%, and the simulated explosion environment has been completed. The total amount of He consumed is 71 m3. In order to ensure that there is no dead angle for ventilation, the He concentration distribution at 1680s is as shown in Fig. 6.

According to Fig. 5, when t = 1680s, the He concentration of sampling points in the calculation model reaches more than 70%, and the simulated explosion environment has been completed. The total amount of He consumed is 71m3. In order to ensure that there is no dead angle

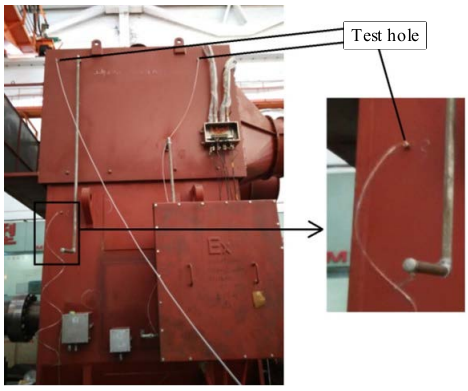

(a) Concentration test point

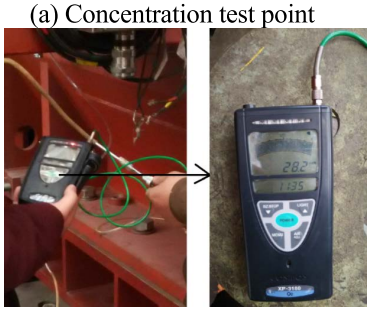

(b) Concentration measurement

FIGURE 4. Explosion-proof concentration measurement test.

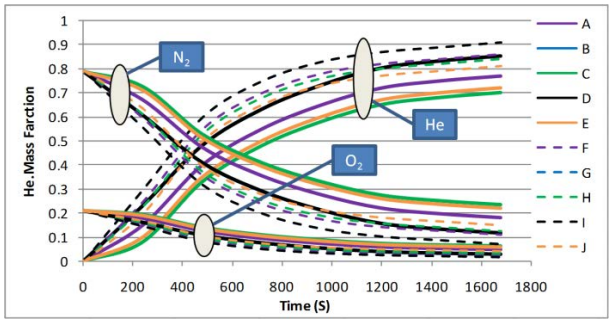

FIGURE 5. The time-varying curves of each component concentration at different sampling points during simulating explosive environment.

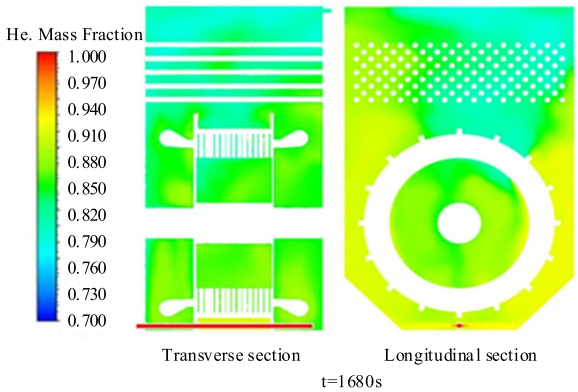

FIGURE 6. The He concentration distribution at 1680s.

for ventilation, the He concentration distribution at 1680s is as shown in Fig. 6.

It can be seen from Fig. 6, the He concentration of the prototype model has reached more than 70%, so as to meet the requirements of the explosive environment.

B. PURGING AND VENTILATION

When t = 1680s, the result data of Fig. 6 is imported into the purging and Ventilation process. When t = 5040s, the He concentration of prototype decreases to less than 1%, the He concentration of prototype is shown in Fig. 7.

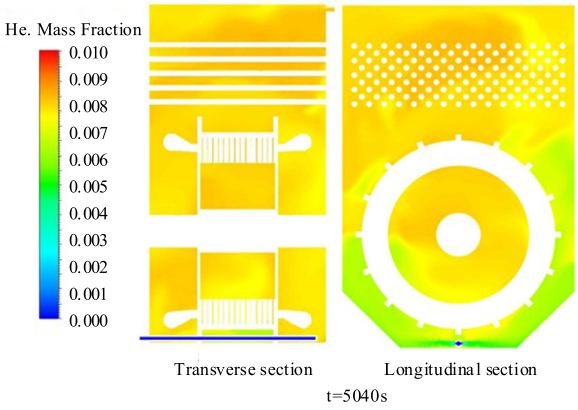

FIGURE 7. The He concentration distribution at 5040s.

The time-varying curves of component concentrations at different sampling points of the motor during the purging transient calculation are shown in Fig. 8.

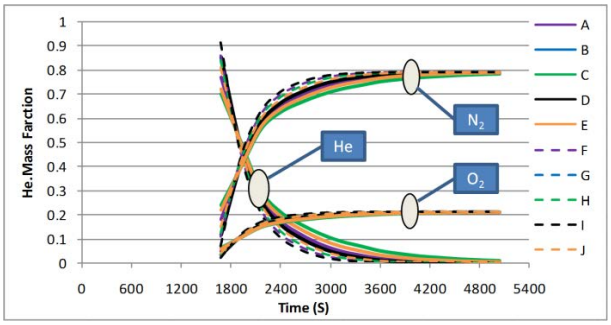

FIGURE 8. The time-varying curves of each component concentration at different sampling points during purging.

According to Fig. 8, when t = 5040s, the concentration of He in all sampling points decreases to less than 1%, and there is no purging dead angle. The purging time is 3360s, and the minimum ventilation volume is 142 m3. It can be seen from the Fig. 6 that the concentration of point C changes slowly, the following work can improve the purging efficiency by optimizing, which can save the test cost, make the motor start-up quickly, and better service conditions.

In order to verify the rationality of the assumptions made, simulations considering fluid friction losses were also carried out for the simulated explosive environment. The temperature of the gas blown into the motor is set to 305K. The remaining parameters and settings of the simulation model remain unchanged. The obtained gas temperature distribution in the motor is shown in the Fig. 9.

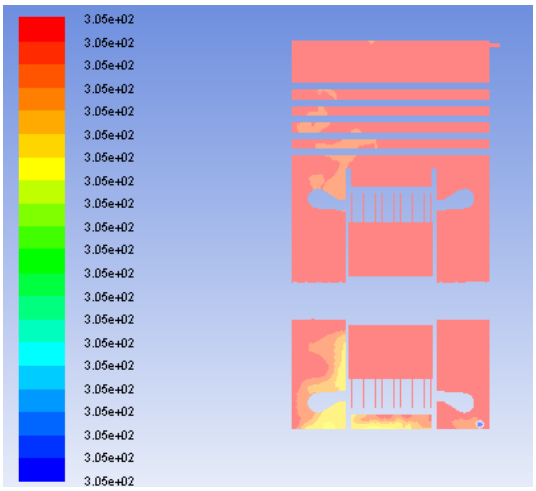

(a) Transverse section

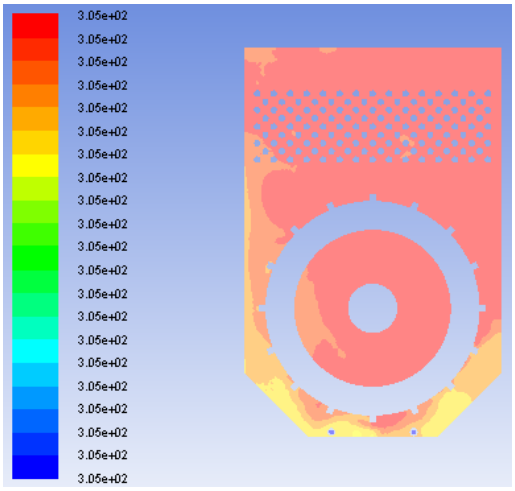

(b) Longitudinal

FIGURE 9. Gas temperature distribution in the motor.

It can be seen from the Fig. 9 that in the process of simulating the explosive environment, the change of gas temperature is minimal. Therefore, the influence of the change of material characteristics caused by the change of gas temperature on the simulation process can be ignored. Similar results were obtained in the simulation during the purging and ventilation process.

C. EXPERIMENTAL COMPARISON

When the concentration of He in all test points reaches 70% or more, and fresh air is purged into the motor. When the concentration of He in all test points decreases to less than 1%, the purging time and the purging volume are recorded. The comparison between experimental and simulation data is listed in Tab. 2.

TABLE 2. The comparison between experimental and simulation data.

	Purging time (min)	Purging volume (m3)
Simulation data	56	142
Experimental data	58	150
Relative error (%)	3.44	5.33

According to Tab. 2, compared with the experimental data, the relative errors of the purging time and the minimum purging volume are 3.44% and 5.33% respectively, which meet the engineering requirements and prove the effectiveness of simulation.

IV. STRUCTURE IMPROVEMENT

A. STRUCTURAL DESIGN

It can be seen from the simulation results that the concentration of He at sampling point C in Fig. 7 is the slowest to decline during the purging process, and the concentration in the middle of the longitudinal section in Fig. 6 is slow to reduce (that is, the concentration in the rotor is slow to reduce). The speed of concentration reduction is mainly related to the arrangement of the intake pipe. Therefore, the intake pipe is improved in Fig. 2, the intake pipe before and after improvement is shown in Fig. 10. After improvement, the opening at the A-end is slightly larger than that at the B-end, which can increase the rate of concentration reduction at the C-point side. Instead, two rows of air intake increase the amount of air intake in the middle and increase the rate of concentration reduction in the middle.

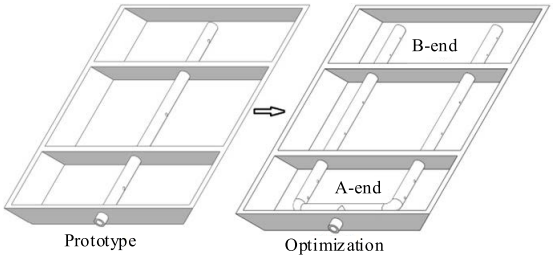

FIGURE 10. Comparison of intake pipes before and after improvement.

B. SIMULATED EXPLOSIVE ENVIRONMENT

The He concentration distribution of the transient calculation of simulated explosive environment when t = 1260s after the improvement of intake pipe is shown in Fig. 10.

According to Fig. 11, the concentration of He at all positions is above 70%. The concentration curve of each component with time in the transient calculation of the simulated explosive environment after the optimization of the intake pipe is shown in Fig. 12.

According to Fig. 12, the time for the He concentration at each sample point to reach the requirement is 1260s,and the total volume of He consumed Q is 53 m3. The rising speed of He concentration at each sample point has also been

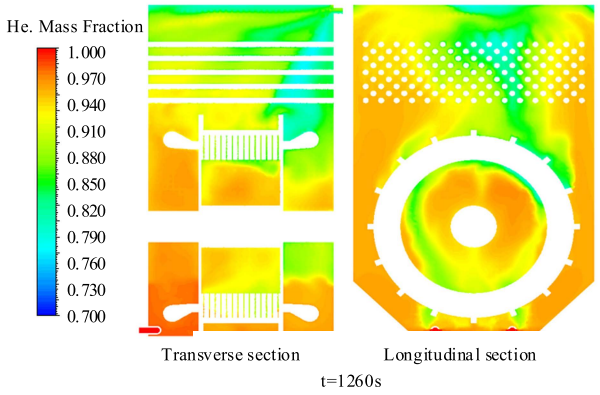

FIGURE 11. The He concentration distribution cloud map after Improvement at t = 1260s.

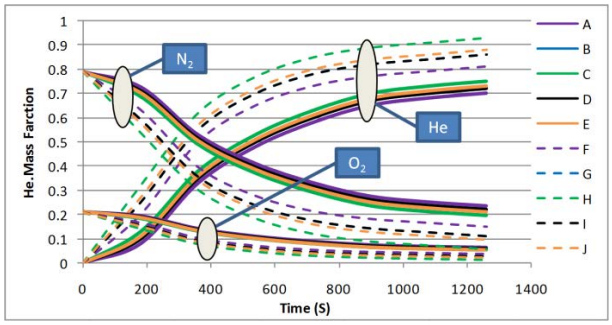

FIGURE 12. The change curve of different components concentration in simulated explosion environment after Improvement.

greatly improved compared to before the improvement and the capacity of He was reduced by 25% compared with that before improvement.

C. PURGING AND VENTILATION

When t = 3780s, the He concentration distribution after the optimization of the intake pipe is shown in Fig. 13. It can be seen from Fig. 13, the He concentration in all positions is reduced to less than 1%, and the purging time is 2520s, which is less than that before the optimization and can greatly improve the purging efficiency At the same time, the speed of concentration reduction in the rotor has been increased, the curve of concentration of each component with time in the transient calculation of purging after optimizing the intake pipe is shown in Fig. 14, it can be seen that the speed of the concentration reduction at point C side has increased significantly.

D. IMPROVEMENT CONTRAST

The reasonable arrangement of purging pipelines can save a lot of purging resources and time. The data comparison before and after improvement is listed in Tab. 3.

According to Tab. 3, compared with the original data, the ventilation and purging effect have increased by 25%, which proves the reasonable arrangement of purging pipeline can

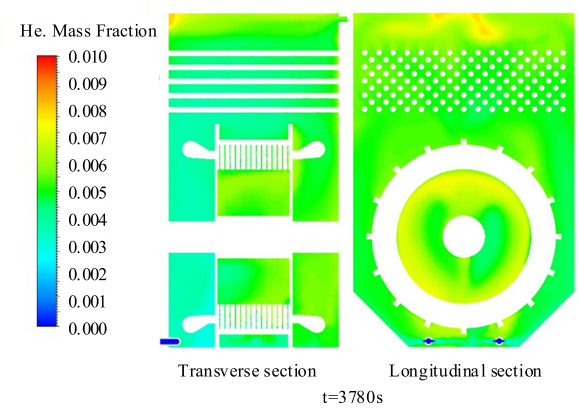

FIGURE 13. The He concentration distribution cloud map after Improvement at t = 3780s.

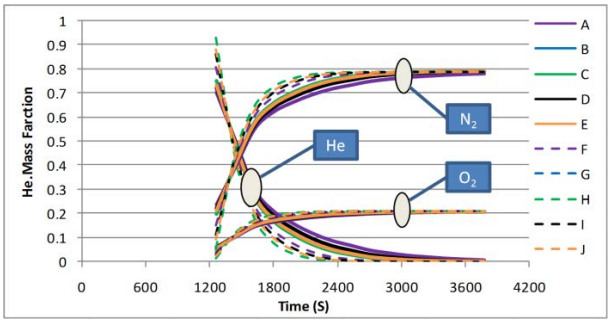

FIGURE 14. Different components concentration change curve during purging after Improvement.

TABLE 3. The data comparison before and after optimization.

	Original model	Optimization model	Promotion effect (%)
Simulated explosive environment time(min)	28	21	25
Simulated explosive environment volume(m3)	71	53	25.35
Purging time(min)	56	42	25
Purging volume(m3)	142	107	24.65

save a lot of purging resources and time, and it also saves a lot of resource to simulated explosive environment.

V. CONCLUSION

Through the research on the safety performance of 6.5 MW positive pressure explosion-proof motor, the following conclusions can be obtained:

(1) Based on the summary of the explosion-proof principle, explosion-proof type, and explosion-proof key technology of the positive pressure explosion-proof motor, the key problem of the research on the safety performance of the positive pressure explosion-proof motor is to simulate the purging process of the motor, which can ensure that the motor can completely exhaust the combustible gas that may exist inside the motor before starting.

(2) Based on the multi-component fluid theory, the purging process of positive pressure explosion-proof motor is simulated by the finite element method, and the purging time and volume are obtained. The simulation results are consistent with the explosion-proof test data, which shows that it is feasible to simulate the purging and Ventilation Progress of the electric machine by the multi-component transient concentration field.

(3) The gas concentration distribution of any position at any time can be obtained by analyzing the concentration nephogram of each part, and whether there is a purge dead angle in the motor can be also known, which enhances the safety of the motor.

(4) Improved the layout of the air intake pipe, which proved that the reasonable layout of the air intake pipe can save the test cost, increase the efficiency of purging, and accelerate the start-up of the motor.

REFERENCES

[1] J. Wen and M. Xu, "Calculation on heat exchange and temperature field in water-cooled explosion-proof motor," *Electr. Mach. Control*, vol. 13, no. 3, 393-397, 2019.
[2] M. D'Souza, I. Malek, and T. Rahill, "API 541 variable speed medium voltage motors applied in a class I, division 1 hazardous location—A case study," *IEEE Trans. Ind. Appl.*, vol. 53, no. 1, pp. 731–738, Feb. 2017.
[3] R. Pokhrel and H. Lee, "Estimation of air pollution from the OGVs and its dispersion in a coastal area," *Ocean Eng.*, vol. 101, pp. 275–284, Jun. 2015.
[4] A. Monteiro, C. Gama, M. Cândido, I. Ribeiro, D. Carvalho, and M. Lopes, "Investigating ozone high levels and the role of sea breeze on its transport," *Atmos. Pollut. Res.*, vol. 7, no. 2, pp. 339–347, Mar. 2016.
[5] J. Zhang, D. Jia, and D. Zhang, "Numerical simulation of exhaust pollution diffusion of motor vehicles in highway tunnels," *Environ. Monitor. Manage. Technol.*, vol. 29, no. 1, pp. 11–15, 2017.
[6] Y. Huang, Z. Liu, and X. Xu, "Influence of building layout on air flow and pollution diffusion in street intersections," *Energy Res. Inf.*, vol. 33, no. 3, pp. 132–137, 2017.
[7] T. Li, "Numerical simulation of air pollution diffusion in residential units," M.S. thesis, Dept. Harbin Inst Technol Liaoning Univ., Harbin, China, 2015, pp. 1–11.
[8] M. Xiao, "Simulation study on the diffusion of radioactive pollutants in nuclear accident," M.S. thesis, Dept. Harbin Inst Technol Liaoning Univ., Liaoning Univ., Shenyang, China, 2015, pp. 1–5.
[9] X. Yu and D. Meng, "Design analysis and improvement of cooler in positive-pressure explosion-proof low-speed high-capacity induction motors," *Appl. Thermal Eng.*, vol. 129, pp. 1002–1009, Jan. 2018.
[10] G. Li and T. Ji, "Severe accidental water vapour explosions in a foundry in China in 2012," *J. Loss Prevention Process Industries*, vol. 41, pp. 55–59, May 2016.
[11] M. Ai, Y. Yang, Y. Xu, Z. Li, L. Xu, and W. Wang, "Research on thermal characteristics of internal ventilated paths in compact medium high-voltage motor based fluid network decoupling," *IEEE Access*, vol. 7, pp. 79268–79276, 2019.
[12] X. Sun, B. Su, S. Wang, Z. Yang, G. Lei, J. Zhu, and Y. Guo, "Performance analysis of suspension force and torque in an IBPMSM with V-shaped PMs for flywheel batteries," *IEEE Trans. Magn.*, vol. 54, no. 11, pp. 1–4, Nov. 2018.
[13] Y. Xu, M. Ai, and Y. Yang, "Research on heat transfer of submersible motor based on fluid network decoupling," *Int. J. Heat Mass Transf.*, vol. 136, pp. 213–222, Jun. 2019.
[14] S. Sun, Y. Qiu, H. Xing, and M. Wang, "Effects of concentration and initial turbulence on the vented explosion characteristics of methane-air mixtures," *Fuel*, vol. 267, May 2020, Art. no. 117103.
[15] L. Pang, Y. Zhao, K. Yang, H. Zhai, P. Lv, and S. Sun, "Law of variation for low density polyethylene dust explosion with different inert gases," *J. Loss Prevention Process Industries*, vol. 58, pp. 42–50, Mar. 2019.
[16] L. Sun, B. Jiang, and F. Gu, "Effects of changes in pipe cross-section on the explosion-proof distance and the propagation characteristics of gas explosions," *J. Natural Gas Sci. Eng.*, vol. 25, pp. 236–241, Jul. 2015.

[17] M. A. Delele, F. Weigler, G. Franke, and J. Mellmann, "Studying the solids and fluid flow behavior in rotary drums based on a multiphase CFD model," *Powder Technol.*, vol. 292, pp. 260–271, May 2016.
[18] S. Chen, "Application of inherent safety explosion-proof technology in oil storage and transportation device," in *Proc. Int. Conf. Adv. Control Eng. Inf. Sci. (CEIS)*, vol. 15, 2011, pp. 4814–4818.

WENHUI LIU was born in Jiamusi, China, in 1983. He is currently pursuing the Ph.D. degree in electrical engineering with the Harbin University of Science and Technology, Harbin, China. He has presided over or participated in ten national, provincial, and departmental scientific research projects and published five academic papers and more than ten patents were obtained. His research interest includes numerical calculation of integrated physical field in motor.

MENGMENG AI was born in Harbin, China, in 1991. He received the Ph.D. degree. He was employed as a Lecturer with the Department of Electrical Engineering, Harbin University of Science and Technology, in 2017. He has presided over or participated in three national, provincial, and departmental scientific research projects and published 15 academic papers (which more than ten papers were included by SCI and EI) and ten patents were obtained. His research interests include optimum design of motor, numerical calculation of integrated physical field in motor, and research on local overheating and fluid field of super large transformer.

LISHEN XU was born in Suihua, China, in 2000. He is currently pursuing the bachelor's degree in electrical engineering with the Harbin University of Science and Technology, Harbin, China. He has participated in a provincial scientific research projects and three patents were obtained. His research interest includes numerical calculation of integrated physical field in motor.

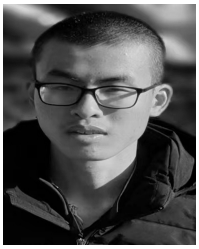

HAN GOU was born in Sichuang, China, in 2000. He is currently pursuing the bachelor's degree in electrical engineering with the Harbin University of Science and Technology, Harbin, China. He has participated in a provincial scientific research projects and one patent were obtained. His research interest includes numerical calculation of integrated physical field in motor.